JBC Papers in Press. Published on December 8, 2008 as Manuscript M807184200
The latest version is at http://www.jbc.org/cgi/doi/10.1074/jbc.M807184200

DEMONSTRATION THAT COBG, THE MONOOXYGENASE ASSOCIATED WITH THE RING CONTRACTION PROCESS OF THE AEROBIC COBALAMIN (VITAMIN B_{12}) BIOSYNTHETIC PATHWAY, CONTAINS A FE-S CENTER AND A MONONUCLEAR NON-HEME IRON CENTER.

Susanne Schroeder[1]*, Andrew D Lawrence[1]*, Rebekka Biedendieck[1], Ruth-Sarah Rose[1], Evelyne Deery[1], Ross M. Graham[2], Kirsty J. McLean[3], Andrew W. Munro[3], Stephen E J Rigby[3] and Martin J. Warren[1]

1. Protein Science Group, Department of Biosciences, University of Kent, Canterbury, Kent, CT27NJ
2. School of Medicine and Pharmacology (M704), University of Western Australia, Fremantle Hospital, Fremantle, 6160, Western Australia, Australia.
3. Faculty of Life Sciences, Manchester Interdisciplinary Biocentre, University of Manchester, 131 Princess Street, Manchester M1 7DN

* Have contributed equally to this work

Running title: Characterization of CobG

Key words: Fe-S center, non-heme iron, precorrin, corrin, metabolism,

Corresponding author: Martin J. Warren, Protein Science Group, Department of Biosciences, University of Kent, Canterbury, Kent, CT2 7NJ; Telephone number: 01227 824690; email m.j.warren@kent.ac.uk

The ring contraction process that occurs during cobalamin (vitamin B_{12}) biosynthesis is mediated via the action of two enzymes, CobG and CobJ. The first of these generates a tertiary alcohol at the C-20 position of precorrin-3A by functioning as a monooxygenase, a reaction that also forms a gamma lactone with the acetic acid side chain on ring A. The product, precorrin-3B, is then acted upon by CobJ, which methylates at the C-17 position and promotes ring contraction of the macrocycle by catalyzing a masked pinacol rearrangement. Here, we report the characterization of CobG enzymes from *Pseudomonas denitrificans* and *Brucella melitensis*. We show that both contain a [4Fe-4S] center as well as a mononuclear non-heme iron. Although both enzymes are active *in vivo*, the *P. denitrificans* enzyme was found to be inactive *in vitro*. Further analysis of this enzyme revealed that the mononuclear non-heme iron was not reducible and it was concluded that it is rapidly inactivated once it is released from the bacterial cell. In contrast, the *B. melitensis* enzyme was found to be fully active *in vitro* and the mononuclear non-heme iron was reducible by dithionite. The reduced mononuclear non-heme was able to react with the oxygen analogue NO, but only in the presence of the substrate precorrin-3A. The cysteine residues responsible for binding the Fe-S center were identified by site-directed mutagenesis. A mechanism for CobG is presented.

INTRODUCTION.

Vitamin B_{12} is the antipernicious anemia factor (1) whose isolation was first described over 60 years ago (2,3) and whose subsequent structure determination by X-ray crystallography revealed that it is a cobalt-containing modified tetrapyrrole (4). As such it belongs to the same family of compounds as heme, chlorophyll, siroheme and coenzyme F_{430} (5). The major structural differences between vitamin B_{12} and these other family members include the shrunken macrocyclic ring that represents the corrin ring component of the vitamin and the presence of upper and lower axial ligands for the centrally chelated metal ion. There has been some considerable interest in the biosynthesis of vitamin B_{12} as there are no chemical or biological parallels for the removal and extrusion of the integral *meso* carbon ion that is required for the contraction of the macrocycle (6).

The coenzyme form of vitamin B_{12} is adenosylcobalamin (Figure 1), which is synthesized by one of the most elaborate and complex biosynthetic pathways known in biological systems requiring somewhere around thirty enzymatic steps for its complete *de novo* synthesis (5). Cobalamin biosynthesis is further complicated by the presence of two similar though biochemically distinct pathways that are referred to as the aerobic and anaerobic routes (7-10). These pathways differ in their requirement for molecular oxygen and the timing of cobalt insertion. The

aerobic pathway requires molecular oxygen to facilitate the ring contraction process prior to cobalt insertion, whereas on the anaerobic route there is no requirement for oxygen but early cobalt insertion is an essential prerequisite for ring contraction.

Along the aerobic pathway for cobalamin biosynthesis, the ring contraction process is mediated by two enzymes called CobG and CobJ (11,12) (Figure 1). Initially, CobG hydroxylates the C-20 position of precorrin-3A and generates a gamma lactone structure with the acetate side chain of ring A to give precorrin-3B (13). CobG utilizes molecular oxygen, which was first shown when it was demonstrated that the enzyme was inactive under anaerobic conditions (12). It was only when the enzyme was incubated with precorrin-3A in the presence of air that any activity was observed. Subsequently, elegant labeling experiments with $^{18}O_2$ revealed that one atom of oxygen was incorporated into the C-20 position (14,15). Moreover, the absolute stereochemistry of precorrin-3B was determined, revealing that the C-20 hydroxyl is *cis* to the oxygen terminus of the gamma-lactone at C-1 (16). This reaction prepares the macrocycle for contraction by CobJ via a pinacol type rearrangement. The extruded carbon fragment is eventually lost as acetic acid. These steps are outlined in Figure 1.

Despite the characterization of the reaction catalyzed by CobG, comparatively little is known about the enzyme itself. CobG is a 459 amino acid protein, with a molecular mass of 46 kDa, and displays similarity to nitrite and sulfite reductases (11). Sulfite reductase, which catalyzes the six-electron reduction of sulfite to sulfide, requires both a [4Fe-4S] cluster and siroheme for activity. In this unusual enzyme, the two cofactors are covalently linked through a shared cysteine residue (17-19).

On the basis that purified CobG was found to have a slight coloration and that atomic absorption analysis of the purified protein indicated that it contained 4.6 moles of Fe and 4 moles of S per mole of protein, it was suggested that the protein is likely to contain a [4Fe-4S] center (11). As a monooxygenase, it has been proposed that the reaction may proceed via an enzyme bound Fe(III)-O^- species (9). In this paper, we provide the first biophysical evidence that CobG does indeed contain both a mononuclear non-heme iron as well as a [Fe-S] cluster. We also show that the substrate must bind in close proximity to these metalloprosthetic groups. Moreover, the cysteine residues required for Fe-S formation are confirmed and the presence of the Fe-S center is shown to be essential for catalytic activity of the enzyme.

EXPERIMENTAL PROCEDURES

Chemicals and reagents. Most chemicals were purchased from Sigma. Other materials were provided by the following suppliers: restriction enzymes, modification enzymes and the vector pGEM®-T Easy were from Promega and New England Biolabs UK; chelating-Sepharose fast flow resin was from Amersham Biosciences, Little Chalfont, Bucks, UK; pET3a, pET14b, pLysS and pETcoco2 were from Novagen, Madison, WI; tryptone and yeast extract were from Oxoid, Basingstoke, UK; sodium dithionite was from Roche, Poole, UK; and primers were from Invitrogen, Paisley, UK.

Recombinant DNA techniques. All strains and plasmids used in this study are listed in Table 1. DNA manipulations were performed in *E. coli* JM109 using established laboratory procedures. Plasmid DNA was isolated using the QIAprep® Miniprep kit (QIAGEN). DNA fragments were isolated from 0.7 % (w/v) or 1.0 % (w/v) agarose gels and purified by using the QIAquick Gel Extraction kit (QIAGEN). PCR products were purified by using the QIAquick PCR purification kit (QIAGEN). DNA sequencing was performed at GATC Biotech, Germany.

Cloning of cobG from Brucella melitensis and Pseudomonas denitrificans. *B. melitensis cobG* (*Bmei0715*) was amplified by PCR from genomic DNA from *B. melitensis* strain 16M. Primers contained the restriction sites *Ase*I and *Spe*I (underlined) and the sequences (5'-3') were actattaatatgcgcaacgctccttttccc and actactagttattgatgtcgggcgttcag. The resulting PCR product was ligated into the pGEM®-T Easy vector. The *cobG* insert was excised using the *Ase*I and *Spe*I sites and ligated into the *Nde*I and *Spe*I sites of the vectors pET-14b and pET-3a. The *P. denitrificans cob*G was amplified by PCR using

the plasmid CR427 as a template and was directly cloned into the *Nde*I and *Spe*I sites of pET14b. The sequences of the *cobG* inserts were confirmed by sequencing.

Site directed mutagenesis. Site directed mutagenesis was performed using the QuikChange® II XL Site-Directed Mutagenesis Kit (Stratagene) to generate point mutations in the plasmid pRS003. The sequences of the resulting plasmids were confirmed by DNA sequencing. The mutagenic primers used are listed in Table 2.

Recombinant protein overproduction and purification. For protein overproduction, the *E. coli* strain BL21(DE3) pLysS was transformed with the appropriate plasmid. The resulting strain was grown at 37 °C in LB supplemented with ampicillin (100 mg/L) and chloramphenicol (34 mg/L). Once the cell density reached $OD_{600} \approx 0.6$ protein overproduction was induced with the addition of 0.4 mM IPTG and the cells were left to grow overnight at 16 °C before harvesting by centrifugation at 3,500 g for 15 min at 4 ºC (Beckman Coulter, JI30). The pellet was gently resuspended in binding buffer (20 mM Tris-HCl, pH 8.0, containing 0.5 M NaCl, 5 mM imidazole) and the cells were broken either by one passage through a cell disrupter (Stansted Fluid) operating at 12,000 psi or by sonication (Sonics Vibracell Ultrasonic processor). Cell debris was removed by centrifugation at 35,000 g for 20 minutes at 4 ˚C. The resulting supernatant was transferred to an anaerobic glove box (Belle Technology), maintained at less than 2 ppm oxygen, and applied to a metal affinity chromatography column charged with Ni^{2+}. The column was washed with buffer containing 20 mM imidazole before elution with 400 mM imidazole.

In vivo assays. The *in vivo* activity of CobG was determined through complementation using a strain containing all the necessary genes for the production of cobyric acid in *E. coli* with the exception of *cobG*. The wild type and mutant *cobG* genes were excised from the vector pET14b using the *Xba*I and *Hind*III restriction sites and ligated into the *Spe*I and *Hind*III sites of pLysS. An *E. coli* strain containing the plasmid pETcoco2[AIΔGJFMKLEHBNSTRWQ] was transformed with the resulting plasmids and restoration of cobyric acid production was monitored using a quantitative bioassay as described previously (20).

In vitro assays. CobG activity was measured *in vitro* using a coupled multi-enzyme system where the production of hydrogenobyrinic acid (HBA) could be easily monitored. To achieve this, a plasmid (pSS200) was constructed that harbored all the genes necessary for the production of HBA except *cobG*. This plasmid, pSS200, was derived from pED420 and pRS005 by cloning a *Mfe*I/ *Spe*I fragment of pRS005 into pED420, which had been cut with the same enzymes. Cleared lysates of an *E. coli* strain harboring the plasmid pSS200 were incubated with crude extract of strains overproducing CobG in 20 mM Tris-HCl buffer, pH 8.0, containing 100 mM NaCl, 720 µg/mL S-adenosyl-L-methionine (SAM), 120 µg/mL 5-aminolevulinic acid (ALA) and 100 µg/mL NADPH for 18-20 hours under aerobic conditions in the dark at 4 °C.

Preparation of Precorrin-3A. Precorrin-3A was synthesized in a multi enzyme reaction containing HemB, HemC, HemD, CobA and CobI. The proteins were purified from two *E. coli* strains harboring the plasmids pRS004 and pED408 by metal affinity chromatography and transferred to an anaerobic glove box (Belle technology). Oxygen and salts were removed by buffer exchange into 20 mM Tris-HCl pH 8.0 containing 0.1 M NaCl (PD-10). The protein mixture was incubated with 360 µg/mL SAM and 120 µg/mL ALA under anaerobic conditions in the dark at room temperature for 18-20 hours.

Isolation of HBA. HBA was purified in its free acid form by initially heating either incubations or extracts containing the compound to 80 °C for 15 min. The extracts were then applied to a small DEAE-Sephadex column and the HBA eluted in 1 M NaCl. The HBA was quantified by high performance liquid chromatography on a BDS Hypersil C-18 column (4.6 x 250 mm; Thermo Electron Corporation) run on a Agilent 1100 series LC/MSD Trap equipped with a diode array detector and eluted at a flow rate of 1 ml min^{-1} with a gradient of acetonitrile in 1 M ammonium acetate.

Electron Paramagnetic Resonance (EPR) spectroscopy. EPR spectra were obtained using a Bruker ELEXSYS E500 spectrometer operating at

X-band. Temperature control was effected using an Oxford Instruments ESR900 cryostat linked to an ITC503 controller. Experimental conditions were as given in the figure captions. Nitric oxide gas was formed by the reaction of sodium nitrite with $FeSO_4$ (1.2 M) in H_2SO_4 (1.8 M) under anaerobic conditions and collected in a syringe. Nitric oxide gas was injected into a sealed vial (2 mL HPLC vial) containing 300 µL of sample. Samples were incubated for 5 minutes before being transferred into EPR tubes and rapidly frozen in liquid nitrogen.

Redox Potentiometry. Redox titrations were performed in a Belle Technology glove box under a nitrogen atmosphere as described previously (21-23).

RESULTS

For the purpose of this research the CobG proteins from *B. melitensis* and *P. denitrificans* were studied. Details of the cloning of the respective *cobG* genes into suitable expression vectors are given in the experimental section. The cloning allowed the two proteins to be produced recombinantly in *E. coli* as His-tagged fusions.

Purification of recombinant CobG. Purifications of the *P. denitrificans* and *B. melitensis* CobG proteins were achieved by metal affinity chromatography under both aerobic and anaerobic conditions. The purified proteins migrated as a single band with a molecular mass of around 50 kDa when analyzed by SDS PAGE (Figure 2a). Purified fractions containing either CobG protein were dark green-brown in color and exhibited a UV-visible spectrum indicative of an iron-sulfur (Fe-S) protein with a broad absorbance around 415 nm (Figure 2b). Preparations typically exhibited an OD_{400}/OD_{280} ratio between 0.28 and 0.36. When the CobG proteins were purified aerobically, the intensity of the absorbance around 415 nm decreased with time, over a period of a few hours, suggesting that the iron-sulfur center was sensitive to oxygen.

His-tagged CobG is active in E. coli. There are no *cobG* mutants available that can be used in complementation studies. We therefore made a recombinant *E. coli* strain with all the genetic material to allow the biosynthesis of HBA except for *cobG*. HBA is the first stable ring-contracted molecule that is easily isolated from the aerobic pathway. This strain accumulates precorrin-3A as it does not have the capacity to make the C-20 hydroxylated and gamma lactone-containing intermediate, precorrin-3B. However, transformation of this *E. coli* strain with a plasmid containing either the *B. melitensis* or *P. denitrificans cobG* resulted in it being able to make HBA (Figure 2c). This demonstrates that both enzymes are active as recombinant His-tagged proteins within *E. coli*.

The activity of the CobG proteins was also investigated *in vitro*. Here, cell lysates enriched with the enzymes required for uroporphyrinogen III synthesis (HemB, C and D) and all the enzymes for HBA synthesis (CobA, I, H, J, M, F, K, L) except CobG, were incubated with ALA, SAM, NADPH and either the *P. denitrificans* or *B. melitensis* CobG. In the presence of the *B. melitensis* CobG, the assay yielded HBA, which was identified by HPLC and mass spectrometry. In contrast, however, the *P. denitrificans* CobG was found to be inactive. Thus, it would appear that *P. denitrificans* CobG is very unstable once it is released from the intact bacterial cells.

Characterization of P. denitrifcans CobG. The UV-visible absorption spectrum of the purified *P. denitrificans* CobG is characteristic of a Fe-S protein and the broad absorption in the region of 415 nm is indicative of a [4Fe-4S] center (24,25). However, to confirm the presence of a putative Fe-S center and to determine the type of center present ([2Fe-2S], [3Fe-4S] or [4Fe-4S]) an electron paramagnetic resonance (EPR) study was conducted. EPR samples were prepared from CobG that had been purified anaerobically in a glove box and to a concentration of >250 µM. The EPR spectrum of the dithionite reduced CobG, recorded at 15 K, shows features at g = 2.048 and g = 1.927 (Figure 3a). This EPR signal was not observed at 70 K or in oxidized samples, which precludes it being a [2Fe-2S] or [3Fe-4S] center because of the differences in the properties of the delocalized electrons in the two types of cluster. A [3Fe-4S] center is easily discounted as such centers contain an even number of electrons in the reduced state and thus do not give rise to an EPR signal when reduced. Furthermore their EPR spectra are very weakly axial and appear as an

almost isotropic line at g ≈ 2.02 in the oxidized state $[3Fe\text{-}4S]^{1+}$ (26). It is more difficult to distinguish signals arising from $[2Fe\text{-}2S]^{1+}$ and $[4Fe\text{-}4S]^{1+}$, the paramagnetic reduced states of the [2Fe-2S] and [4Fe-4S] clusters. Both give rise to axial, pseudo-axial or rhombic spectra with at least one g value below 2.0 due to g-anisotropy. (27). However, due to the nature of the antiferromagnetic coupling (exchange and double exchange coupling) there are several low-lying energy levels available in the $[4Fe\text{-}4S]^{1+}$ system that do not exist in the $[2Fe\text{-}2S]^{1+}$ system, see (27) for further discussion of energy levels in Fe-S systems. The availability of these energy levels promotes electronic relaxation, leading to very short electron spin relaxation times (28). These relaxation times are so short as to effectively preclude the observation of the $[4Fe\text{-}4S]^{1+}$ signal at temperatures above 40K. Collectively, the measured g values and the observed temperature dependence of the signal allow the spectrum to be safely assigned to a $[4Fe\text{-}4S]^{1+}$ cluster (24,29).

CobG contains a mononuclear non-heme iron center. Since CobG does not contain a bound heme or flavin cofactor it has been speculated that the activation of molecular oxygen by CobG may be achieved through a mononuclear non-heme iron center (9). Using EPR spectroscopy it has been possible to confirm that CobG does indeed contain a bound mononuclear non-heme iron center. The EPR spectrum, which was observed in both the oxidized and dithionite-reduced samples, with g = 4.08 (Figure 3b) is assigned to a high-spin (total spin S = 5/2) monomeric non-heme Fe^{3+} ion in a rhombic ligand field. The EPR line shapes of high spin mononuclear Fe^{3+} centers are dominated by zero field splitting (30). These arise from the effects of the ligand arrangement around the ion on the energies of the five electronic orbitals populated by the unpaired electrons. Different ligand arrangements lift the degeneracy in the energies of these orbitals in different ways, thus zero field splitting is indicative of the ligand geometry at the ion and is very sensitive to changes in this geometry. The zero field splitting is described by two parameters, the axial, D, and rhombic, E, zero field splitting parameters. When E/D ≈ 1/3, indicating a rhombic ligand field, the EPR spectrum consists of a single line at g ≈ 4.3. The line width of the EPR spectrum we observed is somewhat larger than might be expected for a 'typical' mononuclear Fe^{3+} iron center. This may arise from E and D values that give E/D of slightly less than 1/3, deviation from ideal rhombic ligand field, or from heterogeneity in the sample leading to an overlap of many different spectra with slightly different E/D. To be catalytically active the iron center would need to be reduced to Fe^{2+} prior to the binding and activation of dioxygen. However, reduction of the mononuclear non-heme iron, which would be observable as a loss of the EPR signal since Fe^{2+} (S = 2) is EPR silent, could not be achieved using either sodium dithionite, sodium borohydride or ascorbate as the reducing agent. Furthermore, the addition of precorrin-3A or either α-ketoglutarate or pterin, which are known to be cofactors for mononuclear non-heme iron proteins (31), had no effect on the EPR spectra and/or the reduction of the iron center by dithionite. Conversely, by this method it was not possible to determine if any Fe^{2+} was already present in the sample. The lack of reducibility of this iron species may explain why the *P. denitrificans* enzyme was found to be inactive when it was assayed *in vitro*.

Midpoint redox potential for the P. denitrificans CobG. The midpoint redox potential for the *P. denitrificans* CobG was determined by redox potentiometry using anaerobic spectroelectrochemical methods, as described in previous studies (21-23). As we have observed recently in studies of the 4Fe-4S center in the PduT protein from *Citrobacter freundii* (32) and also in our work on the *Bacillus megaterium* CbiX protein (33), there are only small changes in the optical spectrum of PduT as the iron-sulfur cluster is reduced from the $[4Fe\text{-}4S]^{2+}$ to the $[4Fe\text{-}4S]^{1+}$ form. Nonetheless, CobG was readily and reversibly titrated between these forms, enabling an accurate determination of the midpoint potential of the cluster as -212 mV (Figure 4).

Characterization of B. melitensis CobG. X-band EPR spectra of purified CobG protein showed no signals under anaerobic conditions. However, taking the sample out of the glovebox and exposing it to air for 10 minutes prior to its EPR analysis gave rise to a signal at g = 4.31 (Figure 5b). This signal is narrow and well defined unlike signals that are normally attributed to adventitious or 'free' iron. It arises from a mononuclear high

spin ferric iron center with a rhombic geometry (30), as described above for the enzyme from *P. denitrificans*. This EPR spectrum is typical of high spin mononuclear none heme Fe^{3+} centers with E/D = 1/3. Despite the presence of oxygen, there is no evidence for the presence of a low spin ferric peroxide species with g values of 2.19, 2.12 and 1.95 (34), or a rhombic O_2 coordinated species with g values of 5.9 and 7.5 (35). Such species have been observed previously in studies of bleomycin and chemical models of mononuclear non heme iron centers, though they are rarely observed in proteins (36)(37). The addition of dithionite to the anaerobic protein gave rise to the spectrum of Figure 5a. This axial spectrum with g values 2.04 and 1.93 was not be observed at 70 K, indicating that it derives from a $[4Fe\text{-}4S]^{1+}$ cluster (27). Thus the enzyme isolated anaerobically possesses a ferrous mononuclear non-heme iron center and a $[4Fe\text{-}4S]^{2+}$ cluster. Although the dithionite-reduced protein contains a $[4Fe\text{-}4S]^{1+}$ cluster and an S=2 high spin ferrous iron, there is no evidence for a strong magnetic interaction between these two centers as the form and behavior of the $[4Fe\text{-}4S]^{1+}$ signal is as expected for an isolated 4Fe-4S center.

The addition of 1-2 equivalents of precorrin-3A to the anaerobically purified protein had no effect on the EPR spectrum. The presence of precorrin-3A did, however, affect both the EPR signals previously observed in its absence and described above, Figure 6a and b. These small but reproducible effects suggest that precorrin-3A does not bind directly to the mononuclear non-heme iron or Fe-S centers. Note that the small but reproducible effect on the mononuclear non-heme iron signal further supports our assertion that this signal arises from a protein-bound mononuclear non-heme iron site and not from adventitiously bound or free iron.

Nitric oxide is an oxygen analogue that forms a paramagnetic iron-nitrosyl species upon binding to a reduced mononuclear non-heme iron (38). Binding of NO to the mononuclear non-heme iron in CobG would provide evidence that this cofactor is indeed the site of oxygen activation. The addition of 5 equivalents of NO to the anaerobic enzyme does not give rise to signals in the g = 4 region (Figure 7a). However, in the presence of precorrin-3A the same concentration of NO does produce a weak signal at g = 4.28, Figure 7b, which is typical of ferro-NO complexes. Such complexes have been observed in protocatechuate 4,5-dioxygenase, lipoxygenase, isopenicillin N-synthase and iron superoxide dismutase (39-42). As with the mononuclear none heme Fe^{3+} signal, the g values and anisotropy of the NO induced signal, which arises from what is effectively a mononuclear non heme Fe^{2+}-NO species, are dependent on the zero field splitting parameters E and D. For a rhombic iron environment in which NO replaces a water molecule or an amino acid residue ligand, the previous studies mentioned above indicate that an isotropic signal at $g \approx 4.3$ would be formed, as we observe. The signal is weak because we are limited in the concentration of NO that we can employ. Too high a concentration damages the iron sulfur cluster, releasing iron and giving rise to a ferro-NO complex in the absence of PC3A. Higher concentrations of NO lead to other signals arising from NO-Fe-S interactions and the loss of the Fe-S cluster. This confirms the presence of a high spin S=2 iron in the anaerobic state since this is a requirement for the formation of the observed iron-nitrosyl, ferro-NO, signal.

Site-directed mutagenesis of CobG. An alignment of several CobG primary sequences reveals a number of conserved residues, including five cysteines (42, 358, 364, 394, 398) and a histidine (390). It seemed likely that four of these cysteines would be involved in the construction of the Fe-S center, although some such centers can use histidine (43). To identify the residues involved in the Fe-S center, all the conserved cysteine and histidine residues were mutated individually to alanine residues using site directed mutagenesis. Constructs encoding the single amino acid substitutions (C42A, C358A, C364A, H390A, C394A and C398A) were generated and the authenticity of the resulting constructs were confirmed by DNA sequencing. The activities of the wild type mutated enzymes were determined in an *in vivo* activity assay. In this assay, an *E. coli* strain producing all the proteins for cobyric acid synthesis but lacking the necessary *cobG*, was transformed with a compatible plasmid containing the *B. melitensis cobG* or one of the mutated *cobG* genes. The results of this assay are shown in Table 3. The *in vivo* assay did not show activity for the

four mutants C358A, C364A, C394A and C398A. Purified protein of these mutants also lacked the characteristic brown color of iron sulfur center-containing proteins, and no EPR spectra could be detected consistent with the presence of a Fe-S center (data not shown). In contrast, the iron-sulfur center remained bound in both the C42A and H390A mutants, as deduced by UV/VIS spectroscopy and EPR, and both these mutant CobG enzymes retained activity in the *in vi*tro assay system. These findings suggest that the cysteine residues in the C-terminus of the protein coordinate the [4Fe-4S] center and that the iron sulfur center plays an important role in the activity of *B. melitensis* CobG.

DISCUSSION

CobG has been successfully overproduced as an N-terminal His-tag fusion protein in *E. coli* and purified by metal affinity chromatography using a column loaded with Ni^{2+}. The UV-visible spectrum of the purified material was indicative of the presence of an iron-sulfur center, which was later confirmed by EPR spectroscopy. The EPR spectrum of the iron-sulfur center was only obtainable after reduction of the protein with dithionite. Significantly, when the temperature was raised from 15 to 70 K the signal disappeared. This marked temperature dependence allowed the signal to be assigned to a [4Fe-4S] center (27). Previously, the presence of this redox center had been implied but never shown experimentally. Site directed mutagenesis suggests that the Fe-S center is formed between four conserved cysteine residues at the C-terminal region of the protein, cysteines 358, 364, 394 and 398. The presence of the Fe-S center appears to be essential for the activity of the enzyme, as demonstrated by our activity complementation and optical studies on the relevant cysteine replacement mutant proteins.

EPR spectroscopy was also used to identify a bound Fe^{3+} mononuclear non-heme iron center in *P. denitrificans* CobG that is a possible site for oxygen activation. In order to bind and activate dioxygen this site would need to be reduced to Fe^{2+}, which is then EPR silent. However, this mononuclear non-heme iron could not be reduced by dithionite or borohydride even in the presence of a wide range of known cofactors for mononuclear non-heme oxygenases or substrate (precorrin-3A). Thus, the center in *P. denitrificans* CobG may be either kinetically/structurally blocked to reduction by these agents, or else have a quite negative reduction potential. In *B. melitensis* CobG the mononuclear non-heme iron site is isolated in the Fe^{2+} oxidation state and the addition of oxygen is required to generate the Fe^{3+} state with a g = 4.31 EPR signal. This signal is very similar to that observed in ferric lipoxygenase and protocatechuate 4,5-dioxygenase (39)(40).The mononuclear non heme Fe^{3+} signal is affected by the addition of precorrin-3A, although the effect is slight, suggesting that it does not arise from direct coordination of the iron by the tetrapyrrole, but rather that precorrin-3A binds close to the mononuclear non-heme iron site as in lipoxygenases (44). Direct binding of substrates or inhibitors to the mononuclear non heme Fe^{3+} center, as is observed in protocatechuate 4,5-dioxygenase, affects the zero field splitting parameters E and D as a new ligand arrangement around the Fe^{3+} ion is created. In protocatechuate 4,5-dioxygenase such binding gives rise to a rhombic spectrum with g = 6.4, 5.5 and 2.0 (40). This is obviously a much larger effect than is observed here. Nitric oxide, which is an oxygen analogue, will form a paramagnetic iron-nitrosyl species upon binding to a Fe^{2+} mononuclear non-heme iron. The EPR spectrum of *B. melitensis* CobG in the presence of low concentrations of NO, however, failed to show an iron-nitrosyl signal. Significantly, though, the addition of precorrin-3A to a sample containing the same concentration of NO did exhibit such an iron-nitrosyl signal at g = 4.28. This suggests that precorrin-3A gates access of NO, and hence also oxygen, to the mononuclear non-heme iron site. Analysis of the peptide sequence of CobG does not reveal any of the typical motifs involving two histidine side chains that have been identified in other iron-containing monooxygenases (45).

The activity of CobG could be detected *in vivo* using a series of *E. coli* strains containing incomplete B_{12} biosynthetic pathways. All attempts to detect enzymatic activity in cell free systems using the *P. denitrificans* CobG, using either cell lysates or the purified enzyme failed. In contrast, the CobG from *B. melitensis* was active

both *in vivo* and *in vitro*. The likely explanation for the difference in activity between the two CobG enzymes is that the *P. denitrificans* CobG contains a sensitive mononuclear non-heme iron that appears to become colloidal once the enzyme is released from the internal environment of the cells. In contrast the *B. melitensis* CobG has a mononuclear non-heme iron that behaves as expected for a cofactor that binds molecular oxygen.

Sequence analysis indicates that CobG has similarity with assimilatory sulfite and nitrite reductases. Sulfite and nitrite reductase both contain [4Fe-4S] clusters that are linked to the iron at the center of the siroheme cofactor through a shared cysteine bridge (Figure 8a). By comparison with CobG, it can be envisaged that precorrin-3A may bind in a similar manner to siroheme, in close proximity to the Fe-S cluster. As indicated by the EPR, the mononuclear non-heme iron is also likely to be located nearby to the bound substrate and the Fe-S center in a position such to promote the formation of precorrin-3B following the activation of oxygen (Figure 8b). A model for the proposed mechanism is illustrated in Figure 8c. Mechanistically, the mononuclear non-heme iron is likely to bind molecular oxygen, which via the addition of an electron from the [4Fe-4S] center will generate a peroxy and then a Fe(III)-O^{+} species. Upon reaction with precorrin-3A, hydroxylation at C-20 occurs, regenerating ultimately the ferrous iron cofactor. Chemical model studies have shown that hydroxylation at C-20, which forms a tertiary alcohol, is an important prerequisite for ring contraction (46).

From an evolutionary perspective, it is probable that sulfite reductases and CobG have arisen through the process of patchwork evolution, where both have retained a shared protein framework yet have specialized to catalyze different processes (47). An alternative enzyme system to CobG is found in some of the Rhodobacteraceae, where a flavoprotein (CobZ) acts as the monooxygenase (48).

In summary, this research has shown that CobG contains both a [4Fe-4S] cluster and a bound mononuclear non-heme iron. Much work is still required to confirm the role of the redox cofactors within the mechanism of this intriguing enzyme.

FOOTNOTES

Funding from the Biotechnology and Biological Sciences Research Council (BBSRC) is gratefully acknowledged. The *B. melitensis* genomic DNA was a generous gift from Jean-Jacques Letesson, Facultes Universitaires Notre-Dame de la Paix, Belgium. The plasmid pCR427 was a generous gift from Dr Charles Rossener (Texas A & M University).

The abbreviations used are: HBA, hydrogenobyrinic acid; ALA, 5-aminolevulinic acid; NO, nitric oxide; SAM, S-adenosyl-L-methionine.

REFERENCES

1. Minot, G. R., and Murphy, W. P. (1983) *JAMA, J. Am. Med. Assoc.* **250**, 3328-3335
2. Rickes, E. L., Brink, N. G., Koniuszy, F. R., Wood, T. R., and Folkers, K. (1948) *Science* **107**, 396-397
3. Smith, E. L. (1948) *Nature* **161**, 638-639
4. Hodgkin, D. C., Pickworth, J., Robertson, J. H., Trueblood, K. N., Prosen, R. J., and White, J. (1955) *Nature* **176**, 325-328.
5. Warren, M. J., Raux, E., Schubert, H. L., and Escalante-Semerena, J. C. (2002) *Nat. Prod. Rep.* **19**, 390-412
6. Battersby, A. R. (1994) *Science* **264**, 1551-1557.
7. Blanche, F., Thibaut, D., Debussche, L., Hertle, R., Zipfel, F., Müller, G. (1993) *Angew. Chem., Int. Ed. Engl.* **32**, 1651-1653
8. Raux, E., Schubert, H. L., Roper, J. M., Wilson, S. W., and Warren, M. J. (1999) *Bioorg. Chem.* **27**, 100-118
9. Roessner, C. A., Santander, P. J., and Scott, A. I. (2001) *Vitam Horm* **61**, 267-297
10. Scott, A. I. (1994) *Heterocycles* **39**, 471-476
11. Debussche, L., Thibaut, D., Cameron, B., Crouzet, J., and Blanche, F. (1993) *J. Bacteriol.* **175**, 7430-7440.
12. Scott, A. I., Roessner, C. A., Stolowich, N. J., Spencer, J. B., Min, C., and Ozaki, S. I. (1993) *FEBS Lett.* **331**, 105-108
13. Debussche, L., Thibaut, D., Danzer, M., Debu, F., Frechet, D., Herman, F., Blanche, F., and Vuilhorgne, M. (1993) *J. Chem. Soc. Chem. Commun.* 1100-1103
14. Spencer, J. B., Stolowich, N. J., Roessner, C. A., Min, C. H., and Scott, A. I. (1993) *J. Am. Chem. Soc.* **115**, 11610-11611
15. Spencer, J. B., Stolowich, N. J., Santander, P. J., Pichon, C., Kajiwara, M., Tokiwa, S., Takatori, K., and Scott, A. I. (1994) *J. Am. Chem. Soc.* **116**, 4991-4992
16. Stolowich, N. J., Wang, J. J., Spencer, J. B., Santander, P. J., Roessner, C. A., and Scott, A. I. (1996) *J. Am. Chem. Soc.* **118**, 1657-1662
17. Christner, J. A., Munck, E., Janick, P. A., and Siegel, L. M. (1981) *J. Biol. Chem.* **256**, 2098-2101
18. Crane, B. R., Siegel, L. M., and Getzoff, E. D. (1995) *Science* **270**, 59-67
19. Janick, P. A., and Siegel, L. M. (1982) *Biochemistry* **21**, 3538-3547
20. Raux, E., Lanois, A., Levillayer, F., Warren, M. J., Brody, E., Rambach, A., and Thermes, C. (1996) *J. Bacteriol.* **178**, 753-767.
21. Dutton, P. L. (1978) *Methods Enzymol* **54**, 411-435
22. Munro, A. W., Noble, M. A., Robledo, L., Daff, S. N., and Chapman, S. K. (2001) *Biochemistry* **40**, 1956-1963
23. Ost, T. W., Miles, C. S., Munro, A. W., Murdoch, J., Reid, G. A., and Chapman, S. K. (2001) *Biochemistry* **40**, 13421-13429
24. Lovenberg, W. (1973) Iron-sulphur proteins. in *Vol II*, Academic Press, New York. pp195-237.
25. Bertini, I., Ciurli, S., and Luchinat, C. (1995) The electronic structure of FeS centers in proteins and models. A contribution to the understanding of their electron transfer properties. in *Structure and Bonding*, Springer, Berlin / Heidelberg. pp 1-53.
26. Johnson, M. K., Duderstadt, R. E. and Duin, E. C. (1999) *Adv. Inorg. Chem*. **47**, 1-82.
27. Mouesca, J. M., and Lamotte, B. (1998) *Coord. Chem. Rev.* **180**, 1573-1614.
28. Bertrand, P., Gayda, J-P, and Rao, K. K. (1982) J. Chem. Phys. 76, 4715-4719.
29. Sweeney, W. V., and Rabinowitz, J. C. (1980) *Annu. Rev. Biochem.* **49**, 139-161.
30. Solomon, E. I., Brunold, T. C., Davis, M. I., Kemsley, J. N., Lee, S. K., Lehnert, N., Neese, F., Skulan, A. J., Yang, Y. S., and Zhou, J. (2000) *Chem. Rev.* **100**, 235-350.

31. Neidig, M. L. and Solomon, E. I, (2005) *Chem. Comm*. 5843-5863.
32. Parsons, J. B., Dinesh, S. D., Deery, E., Leech, H. K., Brindley, A. A., Heldt, D., Frank, S., Smales, C. M., Lunsdorf, H., Rambach, A., Gass, M. H., Bleloch, A., McClean, K. J., Munro, A. W., Rigby, S. E., Warren, M. J., and Prentice, M. B. (2008) *J. Biol. Chem.* **283**, 14366-14375
33. Leech, H. K., Raux, E., McLean, K. J., Munro, A. W., Robinson, N. J., Borrelly, G. P., Malten, M., Jahn, D., Rigby, S. E., Heathcote, P., and Warren, M. J. (2003) *J. Biol. Chem.* **278**, 41900-41907
34. Girerd, J. J., Banse, F., and Simaan, A. J. (2000) *Metal-Oxo and Metal-Peroxo Species in Catalytic Oxidations* **97**, 145-177
35. Simaan, A. J., Banse, F., Mialane, P., Boussac, A., Un, S., Kargar-Grisel, T., Bouchoux, G., and Girerd, J. J. (1999) *Eur. J. of Inorg. Chem.* 993-996
36. Burger, R. M., Peisach, J. and Horowitz, S. B. (1981) *J. Biol Chem*. **256**, 11636-11644.
37. Simaan, A. J., Banse, F., Girerd, J. J., Wieghardt, K, and Bill, E. (2001) *Inorg. Chem*. **40**, 6538-6540.
38. Ryle, M. J., and Hausinger, R. P. (2002) *Curr. Opin. Chem. Biol.* **6**, 193-201
39. Nelson, M. J. (1987) *J. Biol. Chem.* **262**, 12137-12142
40. Arciero, D. M., Lipscomb, J. D., Huynh, B. H., Kent, T. A. and Münck, E. (1983) *J. Biol. Chem*. **258**, 14981-14991.
41. Chen, V. J., Orville, A. M., Harpe, M. R., Frolik, C. A., Surerus K. K., Münck, E. and Lipscomb, J. D. (1989) *J. Biol. Chem*. **264**, 21677-21681.
42. Jackson, T. A., Yikilmaz, E., Miller, A-F. and Brunold, T. C. (2003) *J. Am. Chem. Soc*. **125**, 8348-8363.
43. Bian, S. M., and Cowan, J. A. (1999) *Coord. Chem. Rev.* **192**, 1049-1066
44. Gaffney, B. J. (1996) *Annu. Rev. Biophys. Biomol. Struct.* **25**, 431-459
45. Costas, M., Mehn, M. P., Jensen, M. P. and Que, L, Jnr (2004) *Chem. Rev*. **104**, 939-986.
46. Eschenmoser, A. (1988) *Angew. Chem.* **27**, 5-39
47. Bartlett, G. J., Borkakoti, N., and Thornton, J. M. (2003) *J. Mol. Biol.* **331**, 829-860
48. McGoldrick, H. M., Roessner, C. A., Raux, E., Lawrence, A. D., McLean, K. J., Munro, A. W., Santabarbara, S., Rigby, S. E., Heathcote, P., Scott, A. I., and Warren, M. J. (2005) *J. Biol. Chem.* **280**, 1086-1094

Table 1. Strains and plasmids used in this study
Strain list

Salmonella enterica			
AR3612	*S. enterica Leu+ SmR cysG metE*		(20)
Escherichia coli			
JM109	*end*A1 *rec*A1 *gyr*A96, *thi hsd*R17(r_K-m_k^+) *rel*A1 *sup*E44 Δ(*lac-pro*AB) [F′, *tra*D36 *pro*AB *lac*I^qZΔM15]		Promega
BL21star (DE3)pLysS	F-, ompT, hsdSB (rB-, mB-), dcm, *rne1*31, gal, λ(DE3), pLysS, Cm^r		Invitrogen
BL21 star(DE3)	F^- *ompT hsd*SB ($r_B^-m_B^-$) *gal dcm rne1*31 (DE3)		Invitrogen
List of plasmids			
Plasmid	**Genotype**	**Description**	**Reference or source**
pET3a		cloning vector with T7 promoter	Novagen
pET14b		N-terminal His-tag fusion protein vector with T7 promoter	Novagen
pETcoco2		protein over production vector, regulation of the copy number with glucose and arabinose	Novagen
pLysS		vector expressing the T7 lysozyme	Novagen
pED408	pETcoco2-cobA hemBCD	pETcoco2 vector carrying *M. bar cobA-Mth hemB-B.m. hemC-D-Mth sirC*	This work
pED418	pETcoco2-cobAIGJMFKLHBNSTQ	pETcoco2 vector carrying all genes for cobyric acid production in *E. coli*	This work
pED420	pETcoco2-cobAI(ΔG)JFMKLEHBNSTRQ	pETcoco2 vector carrying all genes for cobyric acid production in *E. coli* except for *cob*G	This work
pRS004	pET14b-cobI	pET14b *Nde*I /*Spe*I fragment cloned with *RccobI Ase*I/*Spe*I	This work
pRS003	pET14b-cobG	pET14b *Nde*I /*Spe*I fragment cloned with *Bmei0715 Ase*I/*Spe*I	This work
pSS004	pET14b-cobG C42A	pET14b vector carrying *Bmei0715* mutant C42A	This work
pSS005	pET14b -cobG C358A	pET14b vector carrying *Bmei0715* mutant C358A	This work
pSS006	pET14b -cobG C364A	pET14b vector carrying *Bmei0715* mutant C364A	This work
pSS007	pET14b -cobG H390A	pET14b vector carrying *Bmei0715* mutant H390A	This work
pSS008	pET14b cobG C394A	pET14b vector carrying	This work

		Bmei0715 mutant C394A	
pSS009	pET14b -cobG C398A	pET14b vector carrying *Bmei0715* mutant C398A	This work
pSS100	pLysS-cobG	pLysS vector carrying *Bmei0715*	This work
pSS101	pLysS-cobG C42A	pLysS vector carrying *Bmei0715* mutant C42A	This work
pSS102	pLysS-cobG C358A	pLysS vector carrying *Bmei0715* mutant C358A	This work
pSS103	pLysS-cobG C364A	pLysS vector carrying *Bmei0715* mutant C364A	This work
pSS104	pLysS-cobG H390A	pLysS vector carrying *Bmei0715* mutant H390A	This work
pSS105	pLysS-cobG C394A	pLysS vector carrying *Bmei0715* mutant C394A	This work
pSS106	pLysS-cobG C398A	pLysS vector carrying *Bmei0715* mutant C398A	This work
pSS200	pET3a-cobAI(ΔG)JFMKLEH	pET3a vector carrying all genes required for hydrogenobyric acid production in *E. coli* with the exception of *cob*G	This work
pRS005	pET3a- cobAIGJFMKLEH	pET3a vector carrying all genes required for hydrogenobyric acid production in *E. coli*	This work
pCR427	pUC18- *cobG*	pUC18 vector carrying *P. denitrificans cobG*	Gift

Table 2. Primers used for site directed mutagenesis. Restriction sites are underlined and the nucleotides exchanged are shown in capital letters.

Primer name	Sequence forward primer	Sequence reverse primer
***Bmelcob*G C42A *Nar*I**	ggcgcagtgcGGCGccAggcctctc	gagaggccTggCGCCgcactgcgcc
***Bmelcob*G C358A *Nhe*I**	cggttgcgcgccGCtAGCggtgcaacg	cgttgcaccGCTaGCggcgcgcaaccg
***Bmelcob*G C364A *Nar*I**	ggtgcaacgggcGCCgcatcggctctg	cagagccgatgcGGCgcccgttgcacc
***Bmelcob*G H390A *Afe*I**	cgatccggtAGCGctAacgggctgtg	cacagcccgtAagCGCTaccggatcg
***Bmelcob*G C394A *Nar*I**	cacctgacgggcGCCgccaaatcctgc	gcaggatttggcGGCgcccgtcaggtg
***Bmelcob*G C398A *Pst*I**	ctgtgccaaatcTGCAgcAgcActtgcc	ggcaagTgcTgcTGCAgatttggcacag

FIGURE LEGENDS

Figure 1. Pathway towards cobalamin biosynthesis. The ring contraction steps of cobalamin biosynthesis, where precorrin-3A is transformed into precorrin-4, are shown. These reactions are catalyzed by CobG and CobJ. The end product of the pathway, adenosylcobalamin, is also shown.

Figure 2. Characterisation of the CobG proteins used in this study.
(a) SDS gel showing the purified *P. denitrificans* and *B. melitensis* CobG proteins. Both proteins migrate with a molecular mass of around 50 kDa.
(b) UV-visible spectrum of *B. melitensis* CobG, where an absorption of around 420 nm is indicative of a [4Fe-4S] center.
(c) Spectrum of HBA synthesized in an *in vitro* assay that contained CobA, I, J, F, M, K, L, E, H and the *B. melitensis* CobG.

Figure 3. X-band EPR spectra of *P. denitrificans* CobG
a) reduced with sodium dithionite and b) as prepared. Experimental parameters: microwave power 0.5mW, modulation amplitude 5G, temperature 15K, average of 2 scans.

Figure 4. Midpoint redox potential of *P. denitrificans* CobG.
The midpoint reduction of the CobG [4Fe-4S] center was determined by spectroelectrochemistry, as described previously (21-23). CobG was reversibly reduced and oxidized (using sodium dithionite as reductant and potassium ferricyanide as oxidant) and spectra recorded at different applied potentials. Small changes in absorption spectrum were observed between the oxidized ($[4Fe\text{-}4S]^{2+}$) and the reduced ($[4Fe\text{-}4S]^{1+}$) forms, manifest as a decrease in spectral intensity in the 400-500 nm region and a small increase in intensity in the 550-650 nm region on reduction. An isosbestic point is located close to 525 nm. The main figure shows a plot of the absorption at 460 nm (close to the position of maximal overall absorption change between oxidized and reduced species) versus the applied potential (mV *versus* the normal hydrogen electrode, NHE). Data were fitted using the Nernst function, yielding a midpoint reduction potential of -212 ± 7 mV. The inset shows the absorption spectra for the oxidized (solid line) and reduced (dashed line) forms of CobG, with arrows indicating direction of absorption change on reduction.

Figure 5. X-band EPR spectra of *B. melitensis* CobG
a) Reduced with sodium dithionite and b) exposed to oxygen. Experimental parameters: microwave power 0.5mW, modulation amplitude 5G, temperature 15K, average of 2 scans.

Figure 6. X-band EPR of *B. melitensis* CobG showing the effect of precorrin-3A binding
a) Dithionite reduced protein and b) oxygen exposed protein. Arrows indicate the regions of the spectra most perturbed by precorrin-3A binding. Experimental parameters: microwave power 0.5mW, modulation amplitude 5G, temperature 15K, each spectrum is the average of 4 scans.

Figure 7. X-band EPR spectra of *B. melitensis* CobG treated with NO.
a) In the absence and b) in the presence of precorrin-3A. Experimental conditions: microwave power 0.5mW, modulation amplitude 10G, temperature 15K, each spectrum is the average of 6 scans.

Figure 8. Model and mechanism of CobG.
Diagram illustrating the coordination and topology of the bound cofactors within sulfite reductase (A) and the putative model of CobG (B). The mechanism is outlined in (C).

Figure 1.

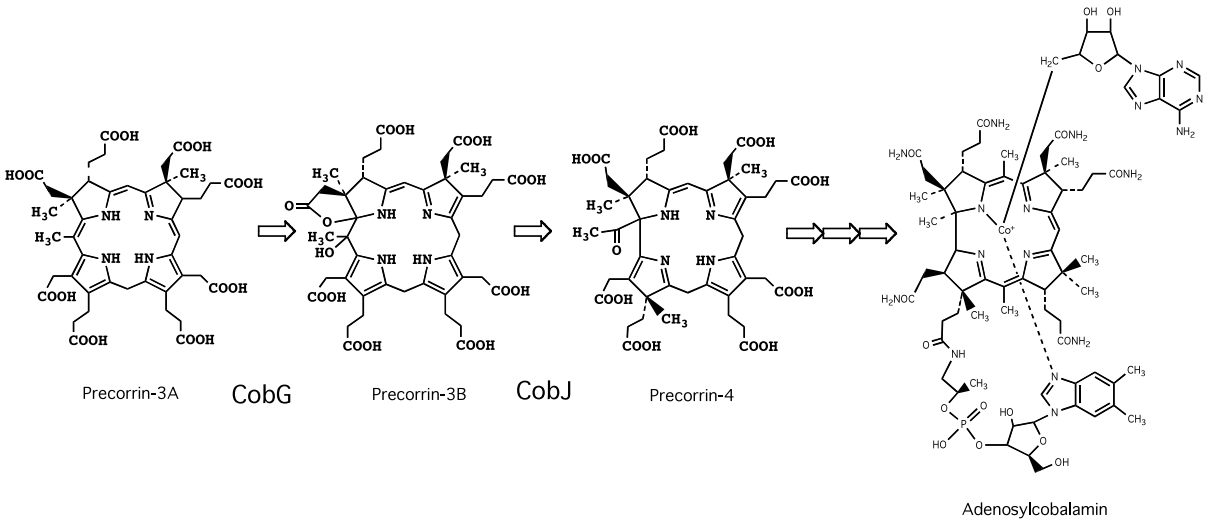

Figure 2

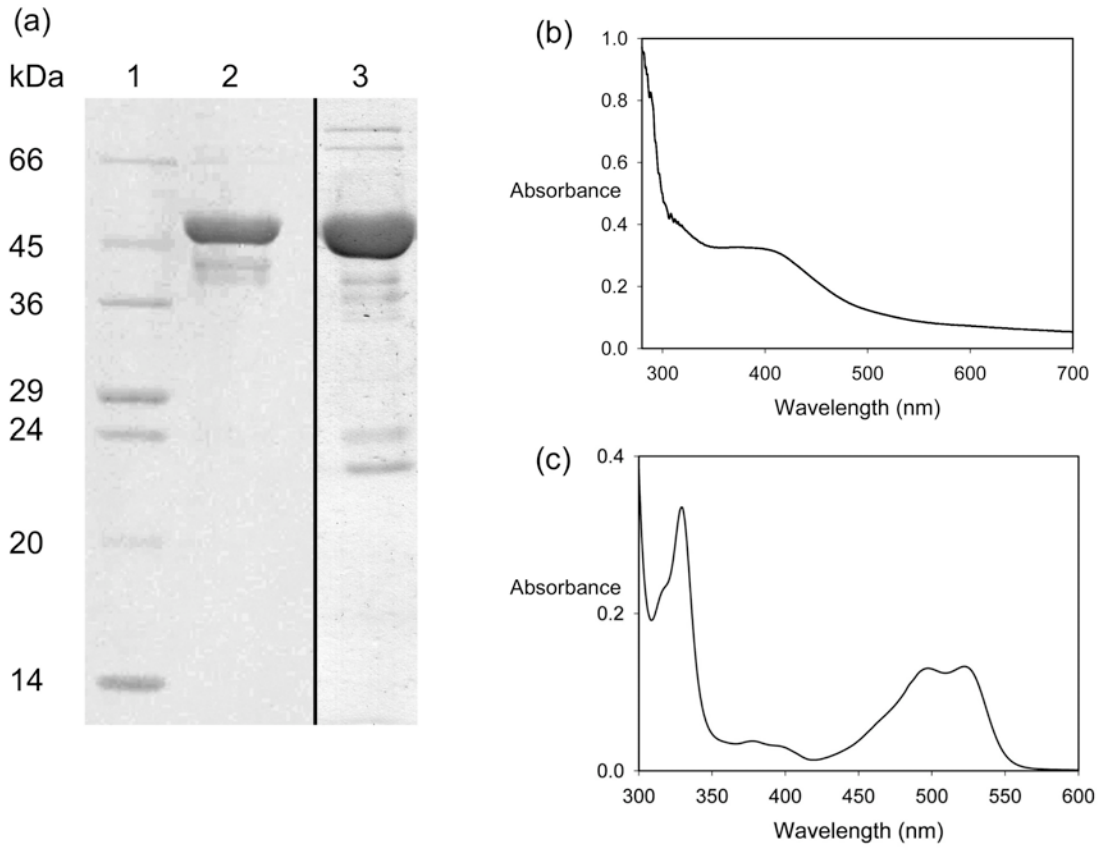

Figure 3.

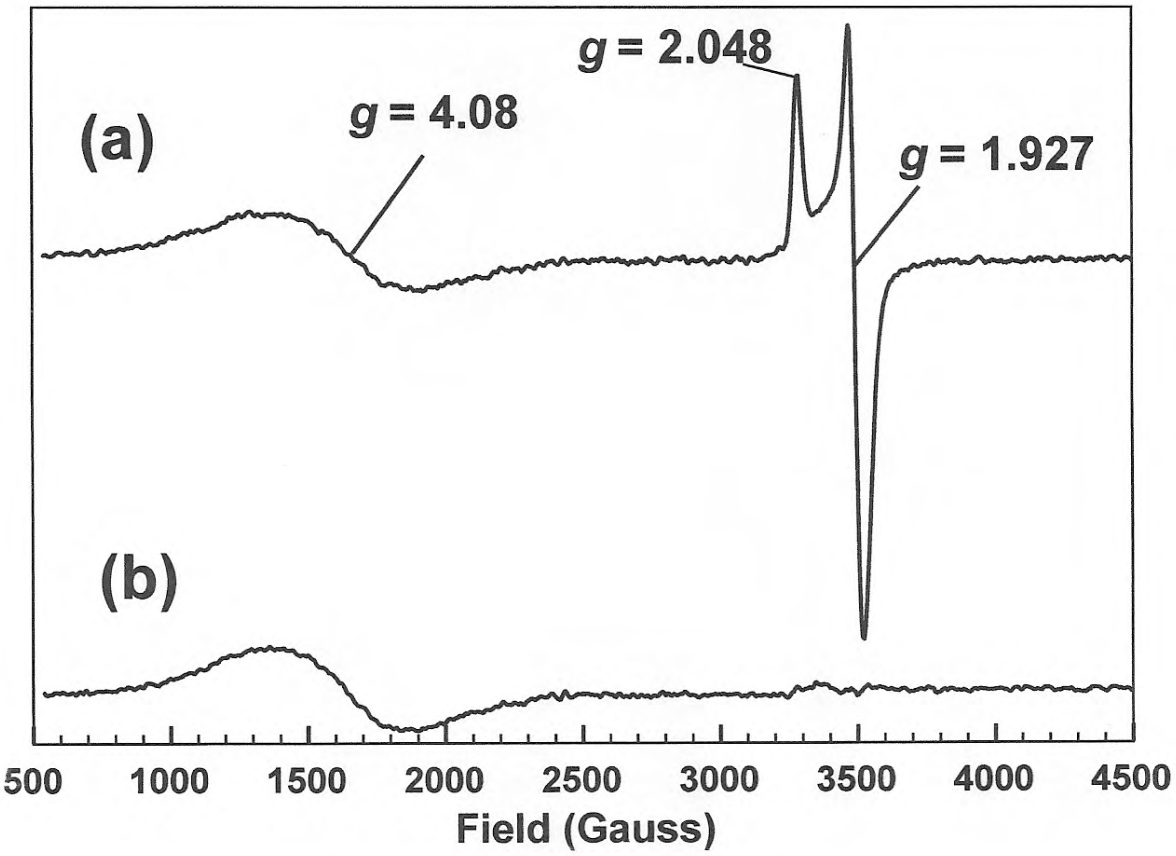

Figure 4.

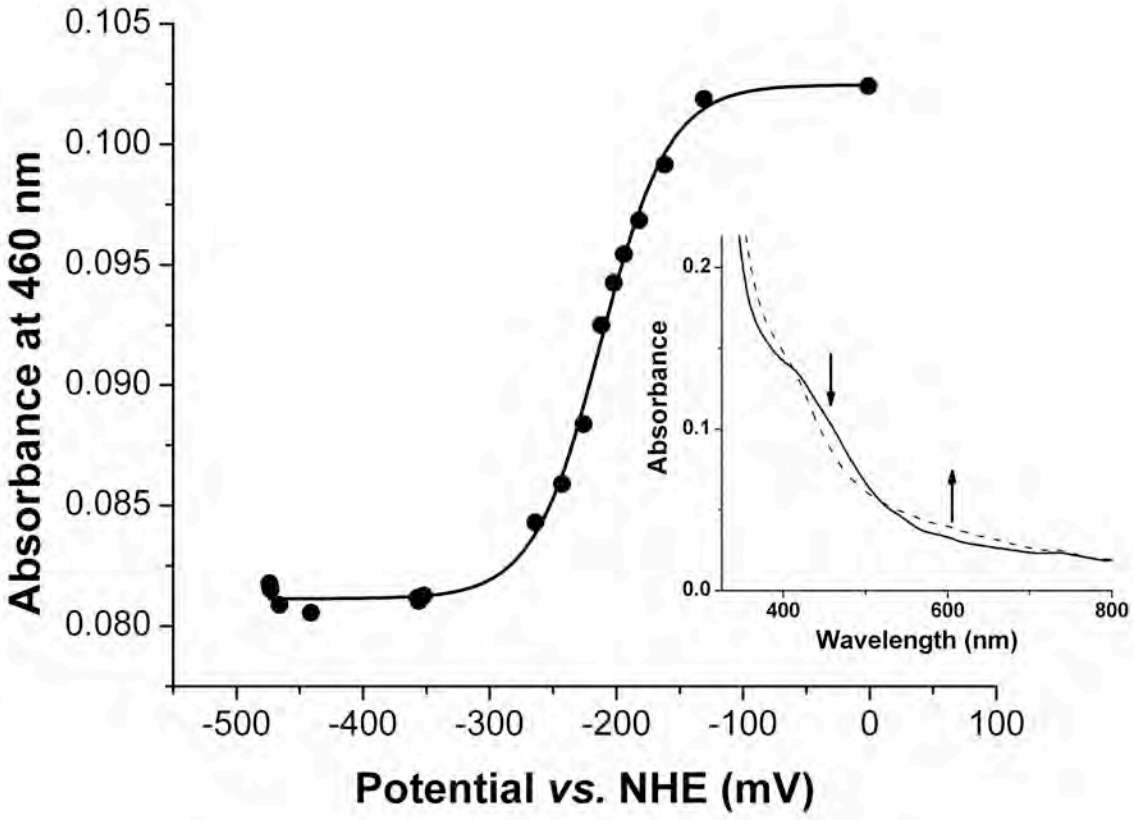

Figure 5.

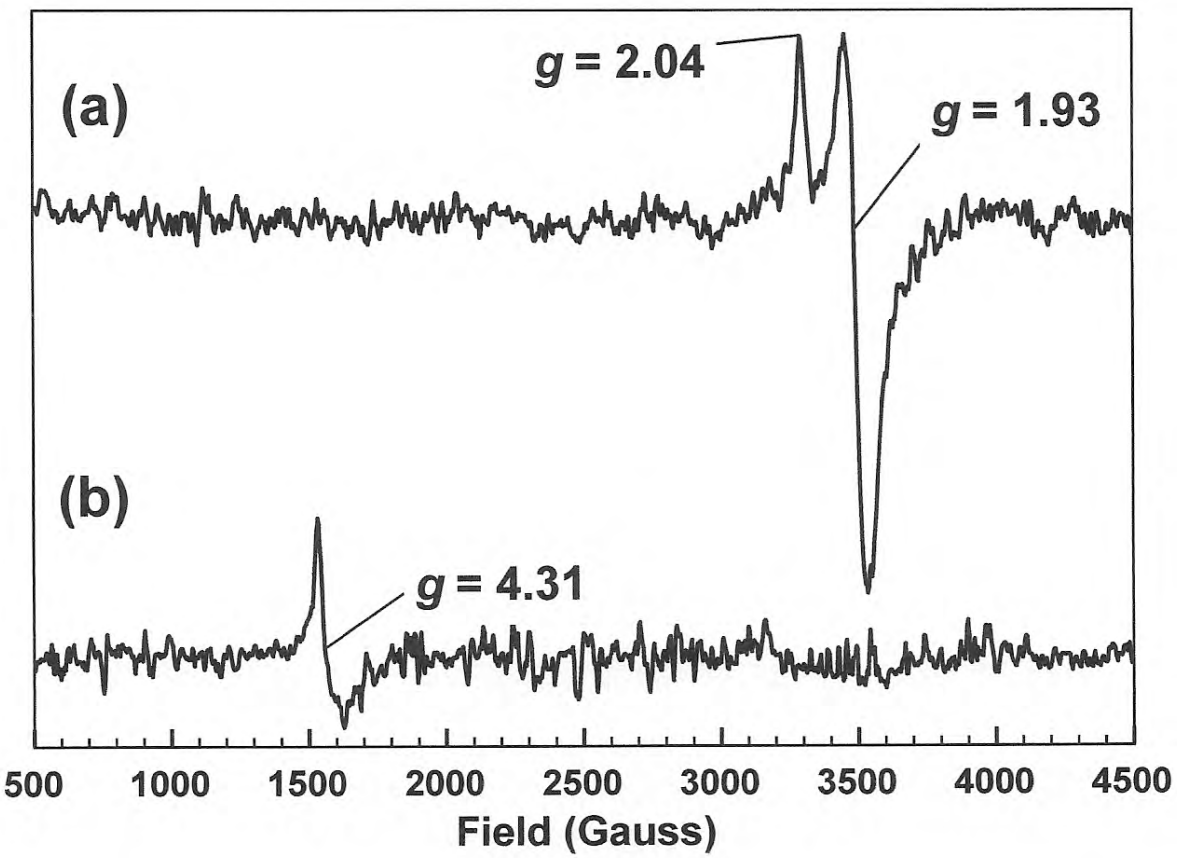

Figure 6.

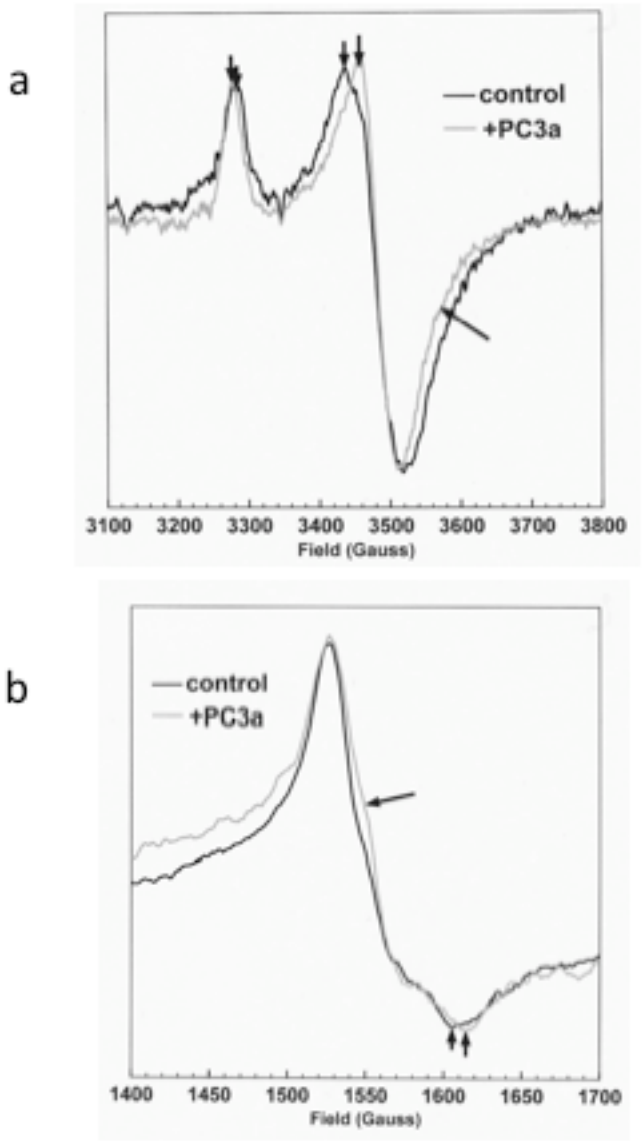

Figure 7.

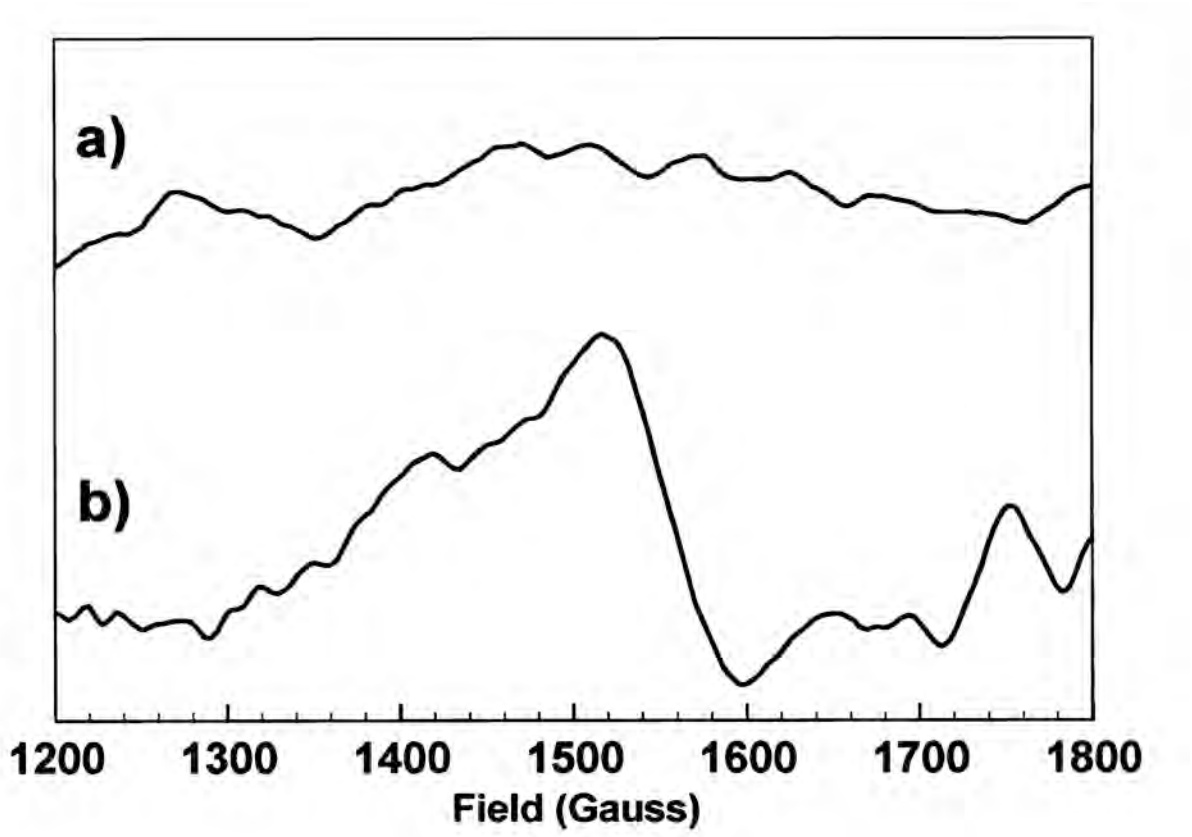

Figure 8

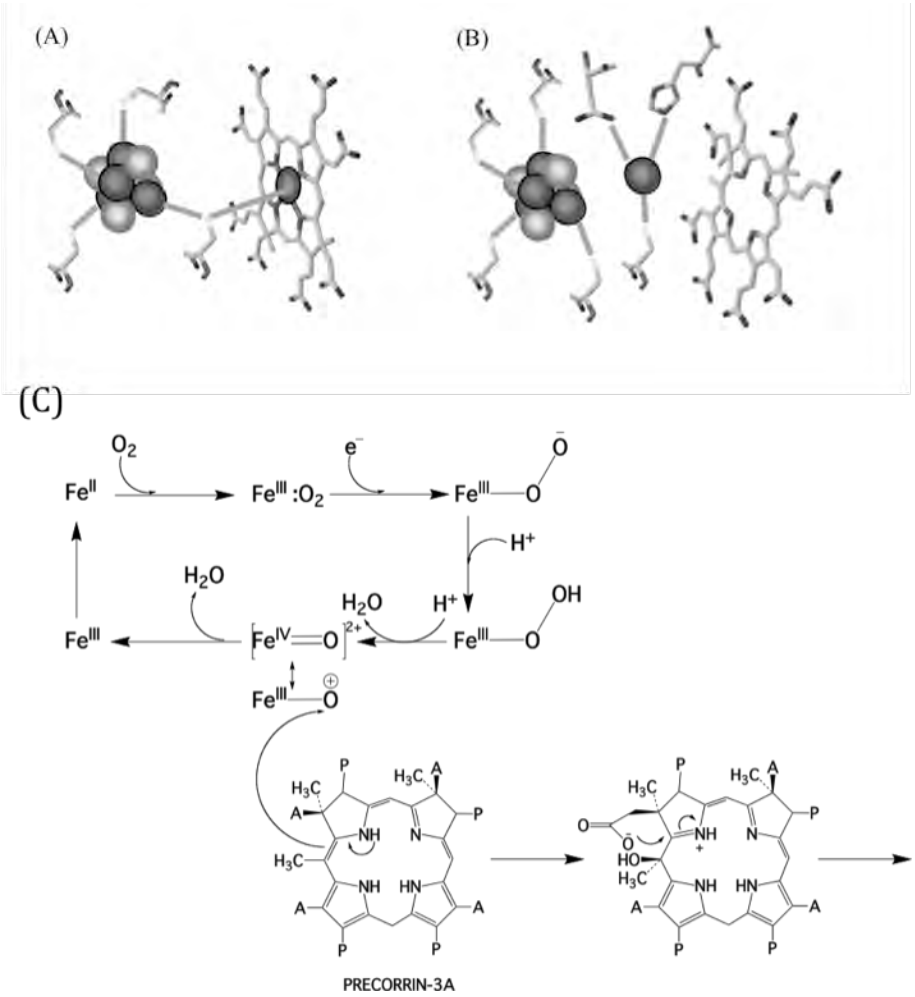

Demonstration that CobG, the monooxygenase associated with the ring contraction process of the aerobic cobalamin (vitamin B12) biosynthetic pathway, contains a Fe-S center and a mononuclear non-heme iron center

Susanne Schroeder, Andrew D. Lawrence, Rebekka Biedendieck, Ruth-Sarah Rose, Evelyne Deery, Ross M. Graham, Kirsty J. McLean, Andrew W. Munro, Stephen E.J. Rigby and Martin J. Warren

J. Biol. Chem. published online December 8, 2008
